Radiation Parameterization in WRF

John Noble

Meteorology 245

December 17, 2007

Outline

- Radiation overview and equations
- Necessity of parameterization
- Historical overview
- Weather Research and Forecasting (WRF) Model radiation schemes
  - Longwave
  - Shortwave
- Gallus and Bresch 2006 study
- Future developments

WRF system components

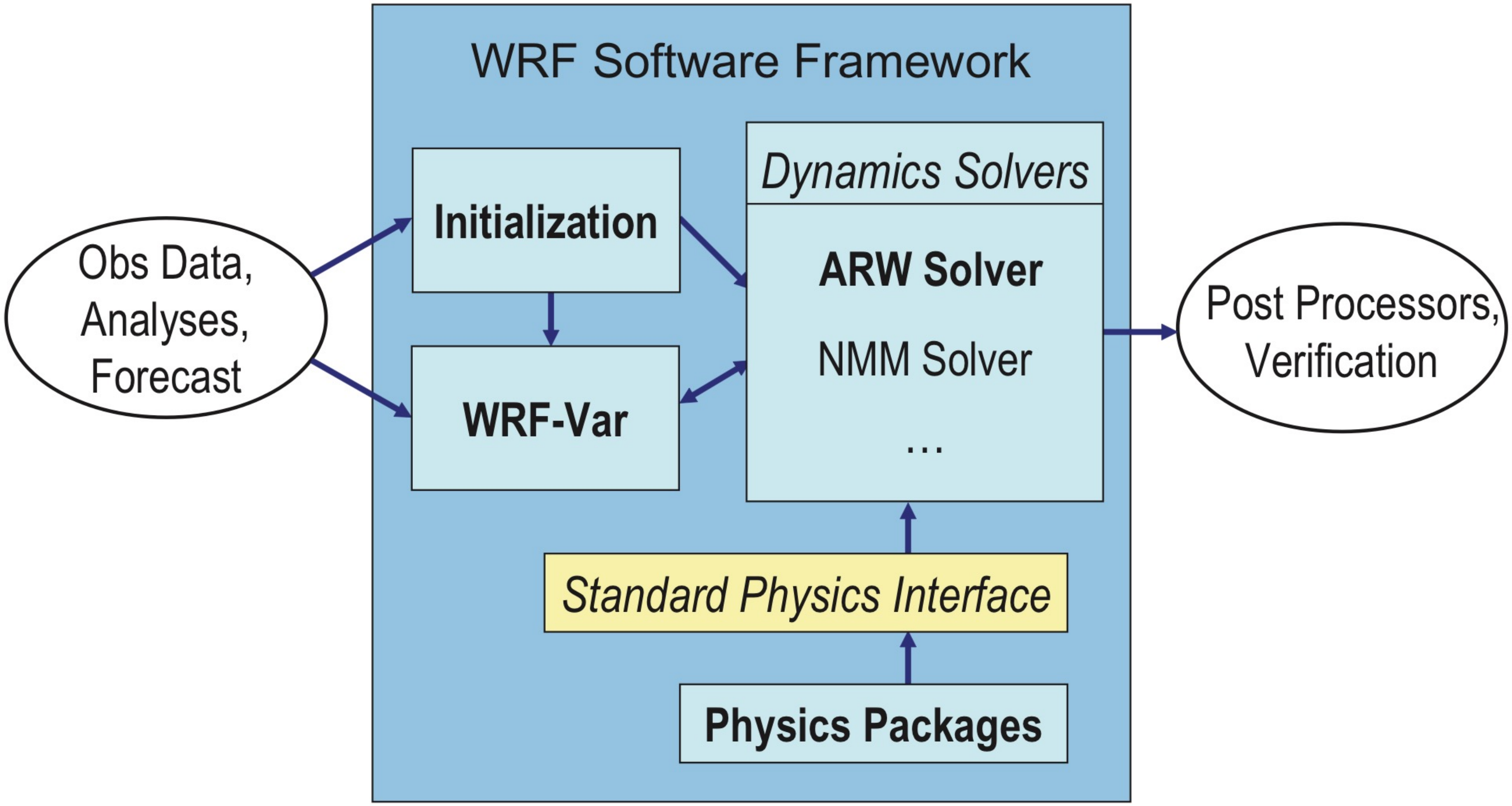

Figure 1.1: WRF system components.

(Skamarock *et al.* 2007)

Schematic diagram of the WRF model

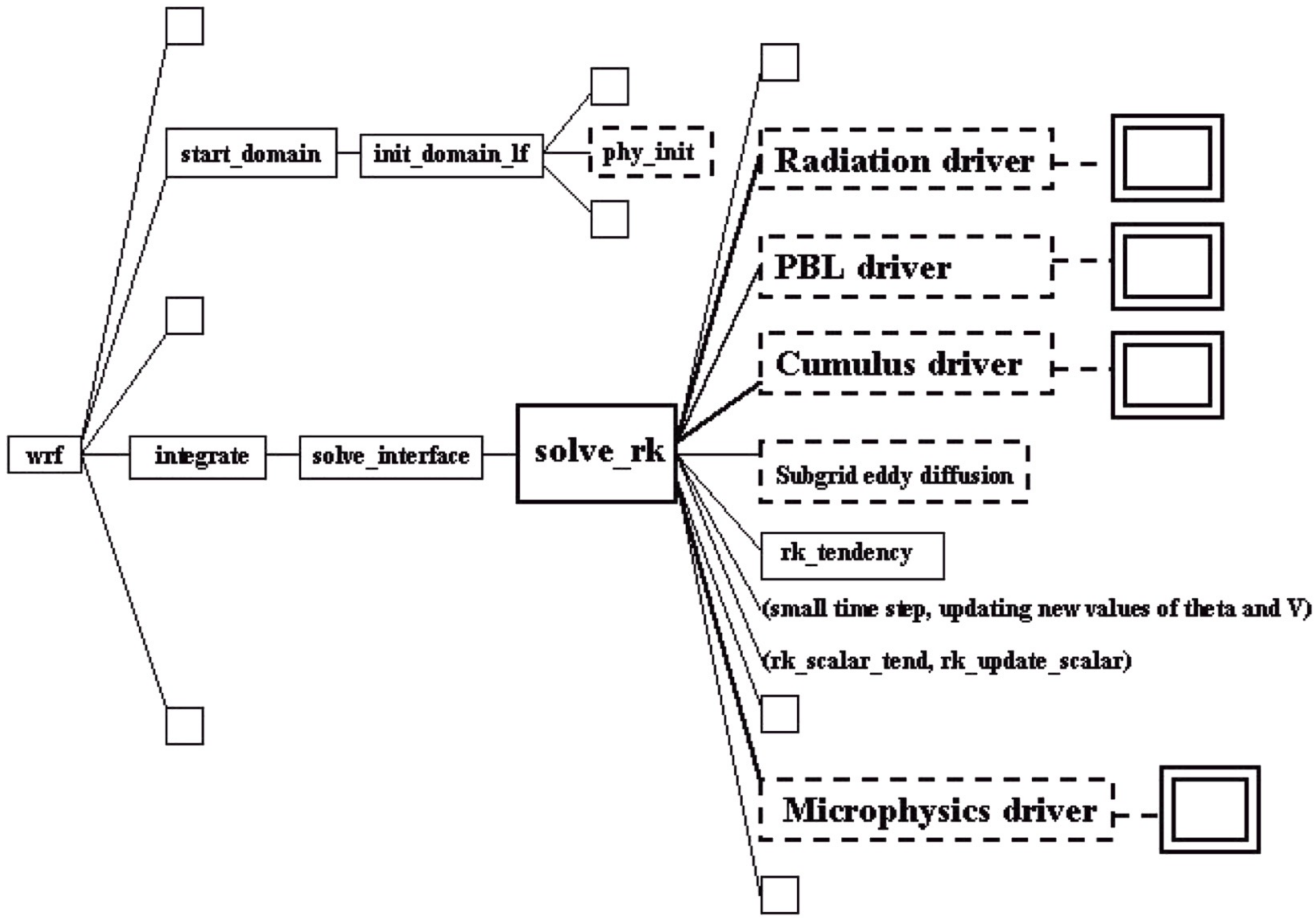

Figure 2: The schematic diagram of the WRF model. wrf is the main program and solve_rk is the major subrouine, which calls dynamics and physics. Dashed-line and double-line (individual scheme) boxes are codes involved with the model physics.

(Chen and Dudhia 2000)

Radiation

- Radiation is propagation of energy by electromagnetic (EM) waves.

- Solar radiation is the fundamental energy source for the Earth and atmosphere, the unequal distribution reaching the Earth leads to differential heating and horizontal gradients that in turn drive atmospheric circulations.

Radiative flux

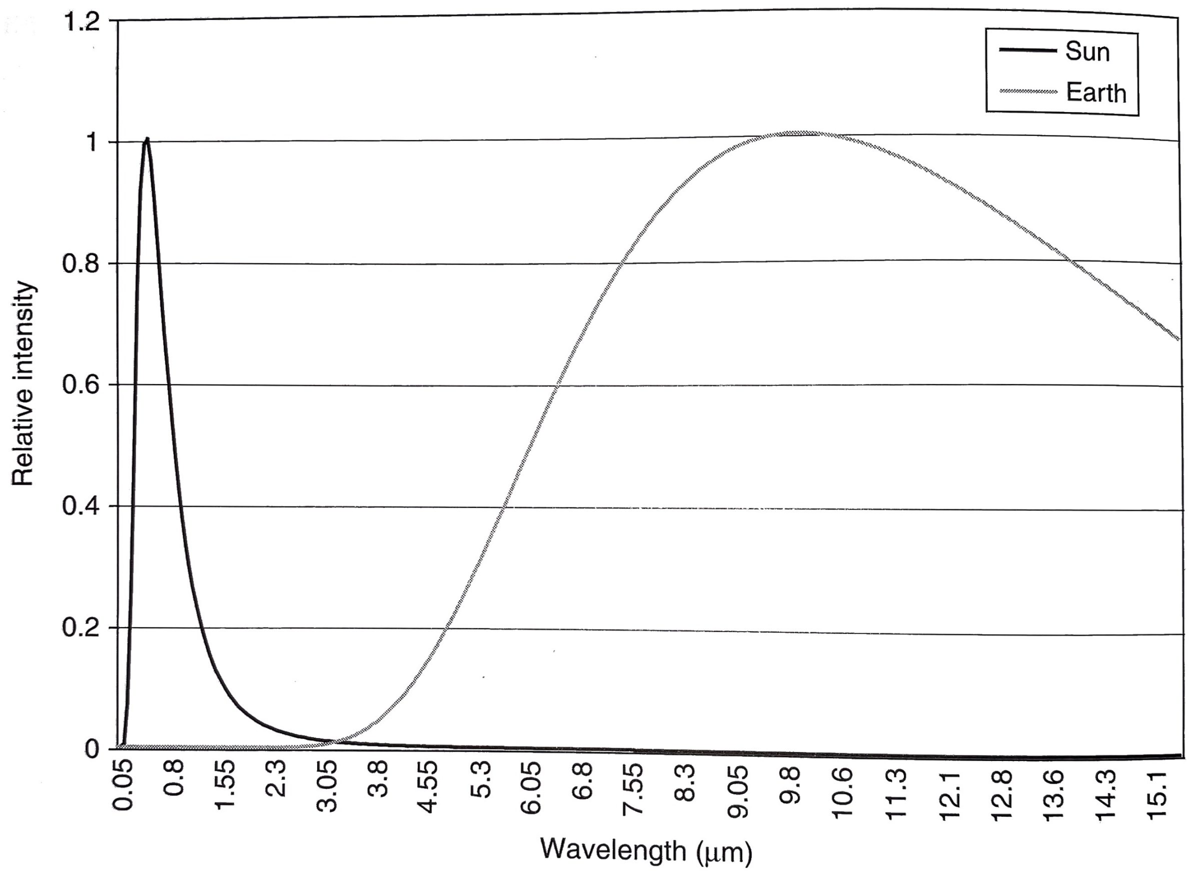

Figure 8.1. Radiative flux calculated using the Planck function and normalized to 1 as a function of wavelength for the sun ($T = 6000$ K, black line) and the Earth ($T = 290$ K, gray line). Note the lack of overlap between the two curves, which allows for the shortwave (sun) and longwave (Earth) components to be treated separately.

(Stensrud 2007)

Solar spectral energy curve

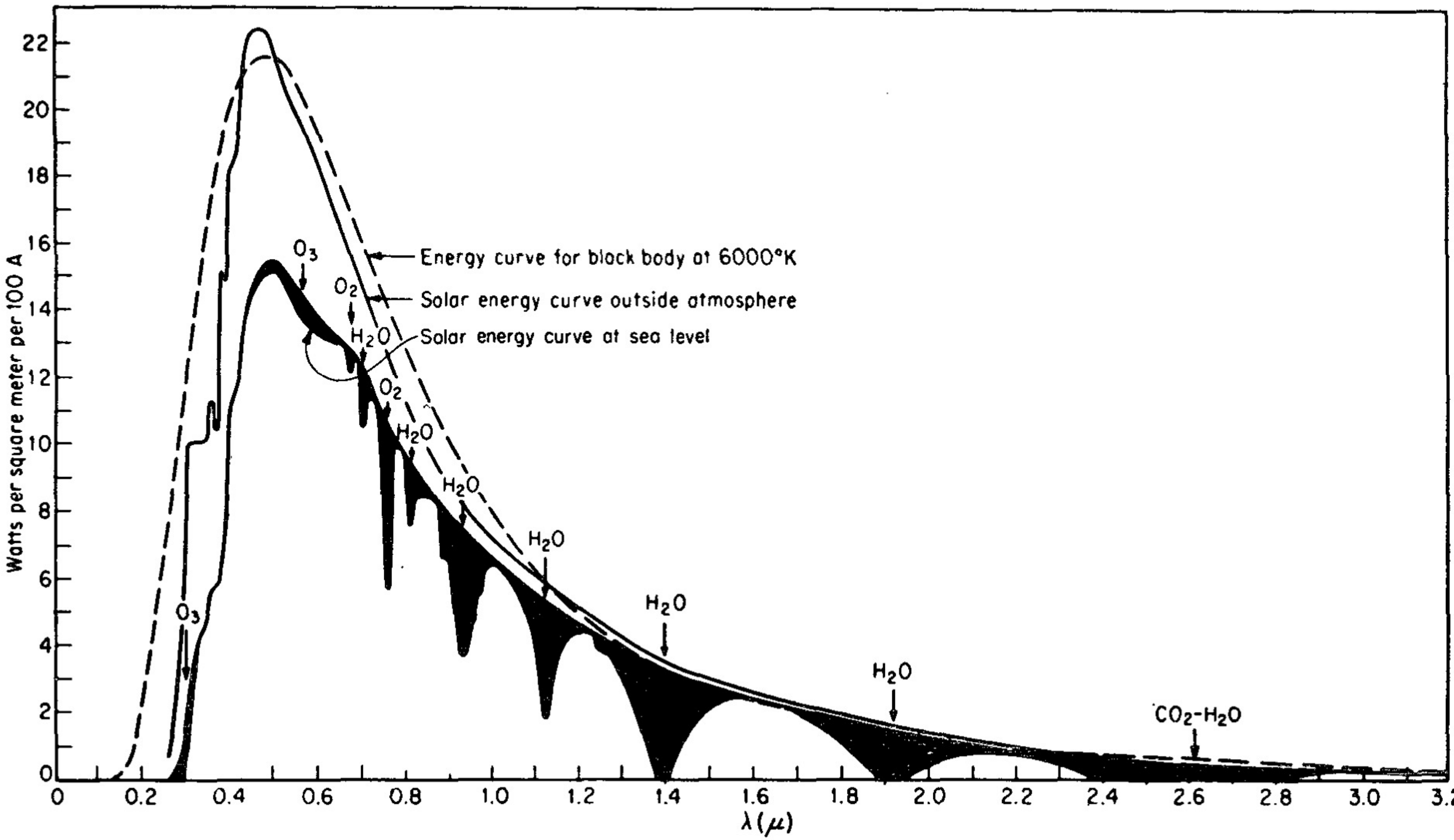

FIG. 1. Spectral energy curve of solar radiation at sea level and extrapolated outside the atmosphere, as given by Pettit (1951). The darkened areas represent gaseous absorption in the atmosphere.

(Lacis and Hansen 1974)

Longwave spectral energy curve

Radiation emitted from the Earth and atmosphere is in the "longwave" (LW) or infrared (IR) band, where λ varies from 4.0 – 25 μm.

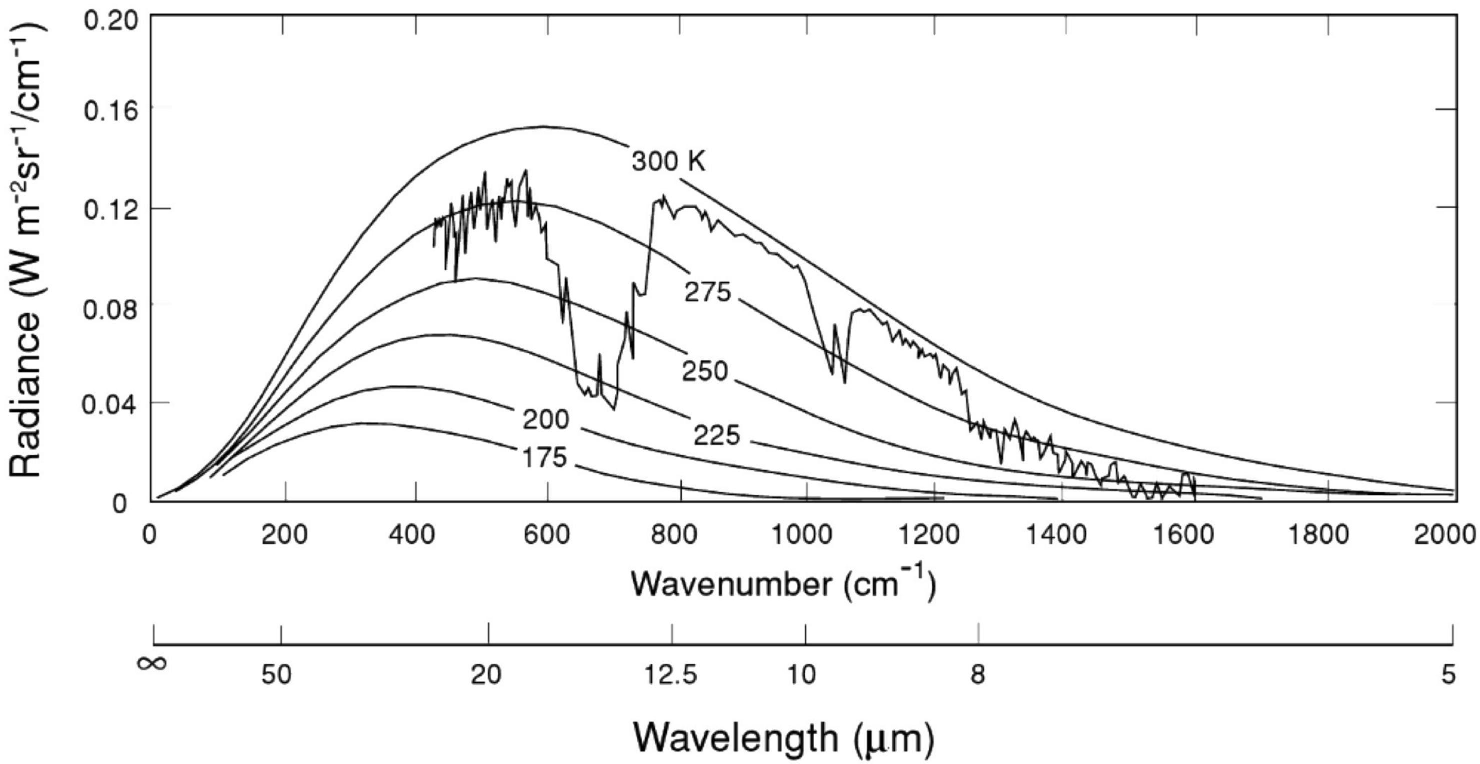

Figure 4.1 Theoretical Planck radiance curves for a number of the earth's atmospheric temperatures as a function of wavenumber and wavelength. Also shown is a thermal infrared emission spectrum observed from the Nimbus 4 satellite based on an infrared interferometer spectrometer.

(Liou 1980; Stensrud 2007)

Blackbody intensity

A blackbody is a theoretical substance that absorbs and emits the maximum possible intensity of radiant energy at a certain wavelength. This intensity was determined by Max Planck as:

$$B_\nu(T) = \frac{2h\nu^3c^2}{\left(e^{hc\nu/K_BT} - 1\right)}$$

Stefan-Boltzman law

Integrating over all wavenumbers yields the blackbody flux density given by the Stefan-Boltzman law:

$$\pi B(T) = \pi \int_0^\infty B_\nu(T)\, d\nu = \sigma T^4$$

Emissivity

Emissivity is given by the ratio of emitted monochromatic intensity to corresponding blackbody radiation:

$$\varepsilon_\lambda = \frac{I_\lambda(\text{emitted})}{B_\lambda(T)}$$

Absorptivity, reflectivity, & transmissivity

Monochromatic absorptivity, reflectivity, and transmissivity are respectively given by:

$$\alpha_\lambda = \frac{I_\lambda(\text{absorbed})}{I_\lambda(\text{incident})},\ R_\lambda = \frac{I_\lambda(\text{reflected})}{I_\lambda(\text{incident})},\ T_\lambda = \frac{I_\lambda(\text{transmitted})}{I_\lambda(\text{incident})}$$

and related by:

$$\alpha_\lambda + R_\lambda + T_\lambda = 1$$

Radiative transfer

Radiative transfer (RT) describes the effects of radiation passing through a medium. The change of monochromatic intensity of radiation passing through the atmosphere is given by:

$$dI_\lambda = -I_\lambda \rho r k_\lambda ds$$

Flux density

The mean flux density of radiation reaching the outer atmosphere is ~1368 W m^{-2} and is given by:

$$F_S = \int_{\delta\omega} I_S \cos\theta \, d\omega$$

and passing through a layer as:

$$F_v^{\downarrow\uparrow}(\tau_v) = 2\pi \int_0^1 I_v^{\uparrow\downarrow}(\tau_v, \mu)\mu \, d\mu$$

Flux transmissivity

The flux transmissivity passing though an atmospheric layer can be formulated as:

$$T_\nu^f = 2\int_0^1 e^{-\tau_\nu/\mu}\mu\, d\mu$$

Necessity of parameterization

- Line-by-line integration of above equations over wavenumber in the IR band is computationally intensive, requiring summation over ~10^6 points

- Thus, the goal of radiation parameterization is to estimate the total radiative flux quickly and accurately, where the total is the sum of surface fluxes and vertical radiant flux density (RFD).

Flux densities

Upward and downward flux densities need to be determined in order to calculate heating/cooling rates for any layer by:

$$\frac{\partial T}{\partial t} = \frac{1}{\rho c_p} \frac{\partial}{\partial z} \left(F_D - F_U \right)$$

Historical overview

There are two general radiation parameterization methods:

1) The first is an empirical approach that relates bulk properties to the radiative flux, essentially estimating downwelling LW radiation at the ground from surface observations.

Empirical approach

This approach is the simplest, computationally cheapest, and least accurate. The inherent assumptions in this approach neglect RFD above the ground and emission from atmospheric gases except water vapor (Stensrud 2007).

Empirical method

- The earliest radiative transfer models were empirical and were accurate only in the clear sky conditions they were designed for (Goody 1952).

- They were unable to make accurate calculations when scatterers were present since they lacked information regarding the absorption coefficient. Rogers and Walshaw (1966) proposed a LW method known as "cooling to space".

Two-stream method

2) The second approach is the two-stream method that solves the LW radiative transfer equations that formulate upward and downward fluxes as a function of height.

$$F_U(z) = \int_0^\infty \pi B_\nu(0)\tau_\nu^f(z,0)\,d\nu + \int_0^\infty \int_0^z \pi B_\nu(z')\frac{d\tau_\nu^f}{dz}(z,z')\,dz'\,d\nu$$

$$F_D(z) = \int_0^\infty \pi B_\nu(z')\frac{d\tau_\nu^f}{dz'}(z,z')\,dz'\,d\nu$$

Two-stream method

- The first term accounts for attenuation of LW radiation emitted from the surface, while the second term accounts for atmospheric contributions (Stensrud 2007; Liou 2002).

- LW parameterization schemes differ as a function of approach to calculate the above integrals (Stensrud 2007).

Two-stream method

- Sasamori (1972) introduced a two-stream method that was later adopted and popularized by Pielke (1984).

- There are several parameterizations that take different approaches to solving the integrals in the full equations (not shown). The first makes a simplifying assumption that eliminates the need to integrate over all viewing angles.

Two-stream method

- The second approach integrates the absorption coefficient over the optical path.

- The third linearly interpolates between stored values for the absorption coefficients that have been calculated over the full range of atmospheric conditions and stored. This approach has higher computational expense than previous (Stresund 2007).

Correlated-*k* method

- The correlated-*k* method provides an alternative to line-by-line integration of RT equations for flux density and transmissivity .

- RT calculations for a given spectral band are performed using a small number of absorption coefficients that are representative of the coefficients for all frequencies in the band.

Correlated-k method

The correlated-k method maps $k(v)$ from spectral space to a space defined by a cumulative probability density function, $g(k)$, where $g(k)$ is the fraction of the individual values of $k(v)$ within the interval delta v with values smaller than k.

The mapping transformation, $v \rightarrow k$, produces a new function, that is monotonic, smooth, and amenable to approximation by summation.

Correlated-*k* method

Transformation of flux transmissivity yields:

$$T_{\bar{\nu}} \equiv \frac{1}{\Delta\nu}\int_{\Delta\nu} e^{-k_\nu u}\, d\nu = \int_0^1 e^{-k(g)\,u}\, dg$$

Correlated-*k* method

Binning the data allows the above equation to be discretized into an approximation

$$T_{\bar{v}} = \sum_{j=1}^{M} e^{-k\left(g_j\right)u} \Delta g_j$$

that reduces the number of calculations by several orders of magnitude.

Absorption coefficients

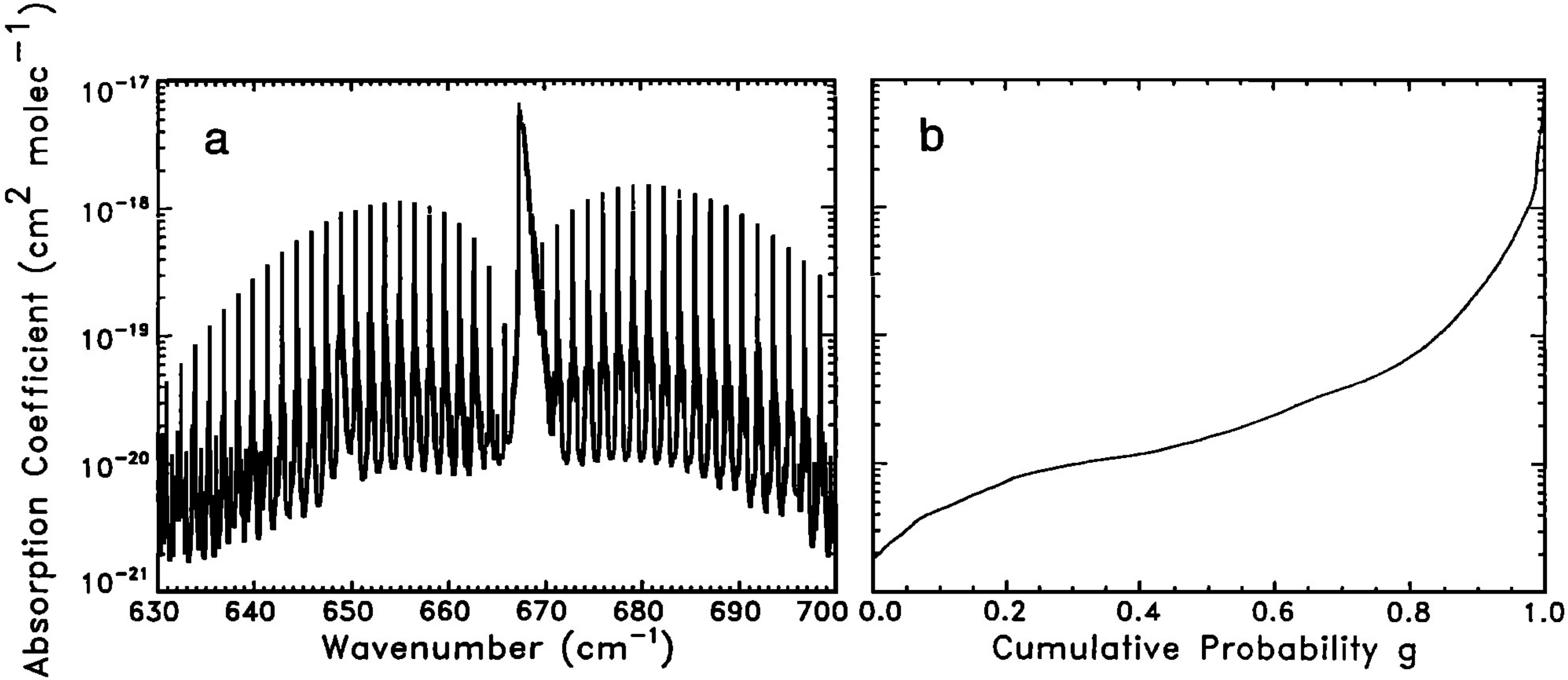

Figure 1. Absorption coefficients due to carbon dioxide for a layer (P = 507 mbar) in the midlatitude summer atmosphere for the spectral range 630–700 cm^{-1} (a) as a function of wavenumber and (b) after being rearranged in ascending order.

(Mlawer *et al.* 1979)

g–space bands & weights

Table 2. Boundaries and Weights of Subintervals in *g* Space Used in RRTM

Subinterval	Initial *g* Value	Final *g* Value	Weight
1	0.00000	0.15275	0.15275
2	0.15275	0.30192	0.14917
3	0.30192	0.44402	0.14210
4	0.44402	0.57571	0.13169
5	0.57571	0.69390	0.11819
6	0.69390	0.79583	0.10193
7	0.79583	0.87911	0.08328
8	0.87911	0.94178	0.06267
9	0.94178	0.98427	0.04249
10	0.98427	0.98890	0.00463
11	0.98890	0.99273	0.00383
12	0.99273	0.99576	0.00303
13	0.99576	0.99798	0.00222
14	0.99798	0.99939	0.00141
15	0.99939	0.99993	0.00054
16	0.99993	1.00000	0.00007

(Mlawer *et al.* 1997)

WRF radiation schemes

- WRF architecture allows use and comparison of various physics algorithms.

- WRF includes two longwave radiation schemes: Rapid Radiative Transfer Model (RRTM) scheme that accounts for multiple bands and trace gases, and GFDL scheme that includes cloud microphysics effects.

- Both utilize look-up tables and provide atmospheric heating from radiative flux divergence.

WRF SW radiation schemes

- WRF includes three SW radiation schemes: Goddard shortwave, GFDL, and simple shortwave schemes, all of which include absorption, reflection, and scattering (Skamarock *et al.* 2007).

- The primary source of SW radiation is solar insolation that can be scattered, reflected, or absorbed. Reflection causes upward fluxes due to surface albedo.

WRF LW radiation schemes

- LW radiation includes IR radiation absorbed and emitted by gases and the surface. Upward LW radiative flux from the surface is determined by its emissivity, a function of surface temperature and land-use type (Skamarock *et al.* 2007).

- Positive RFD relates to the radiative warming rate, while negative relates to the radiative cooling rate. Radiative transfer parameterizations can be the most computationally expensive of all the physical parameterizations.

SW radiation

The factors effecting downward SW flux include:

- the albedo and absorption of clouds, S_{cs}
- solar zenith angle increases path length and reduces $S_{\downarrow}$
- scattering and water vapor absorption in clear air

The combination of these attenuating effects are formulated by:

$$S_d(z) = \mu S_0 - \int_z^{top} \left(dS_{cs} + dS_{ca} + dS_s + dS_a \right)$$

Simple SW radiation scheme

- The simple SW radiation scheme is based on Dudhia (1989) and is taken from MM5. It has downward integration of solar flux that accounts for clear-air scattering, H_2O vapor absorption, and cloud absorption and reflection. It utilizes look-up tables for clouds (Skamarock *et al.* 2007).

- SW radiation reflected upward by clouds and the surface are ignored. SW radiation calculations are performed every 10 minutes.

RRTM LW Scheme

RRTM aims to calculate fluxes and cooling rates comparable with the line-by-line radiative transfer model (LBLRTM), while performing a smaller number of radiative transfer operations.

This is accomplished by use of the correlated-*k* method, with *k*-distributions obtained from LBLRTM (Mlawer *et al.* 1997).

RRTM LW Scheme

LW radiation absorption occurs for H_2O vapor, CO_2, O_3, CH_4, N_2O, CFC-11, CFC-12, CFC-22, and other species. It is necessary to subdivide the LW band into a number of spectral intervals that contain strong absorption due to certain species.

Contributions from the major absorbing species are then determined with a high degree of accuracy, while those from the minor species are determined with a less detailed approach (Mlawer *et al.* 1997).

RRTM LW Scheme

- Radiative transfer calculations are performed for each subinterval in each band. The subintervals are processed in the same way that a spectral point is processed in the LBLRTM.

- The major difference is the number of required calculations: 10^6 spectral points per band vs. 16 intervals in *g*-space per band for LBLRTM and RRTM respectively. RRTM flux and cooling rates are finally compared and validated against those determined from LBLRTM.

RRTM bands

Table 1. RRTM Bands

Band Number	Wavenumber Range, cm^{-1}	Species Implemented in RRTM: Lower* Atmosphere — Key Species	Lower* Atmosphere — Minor Species	Middle/Upper† Atmosphere — Key Species	Middle/Upper† Atmosphere — Minor Species
1	10–250	H_2O		H_2O	
2	250–500	H_2O		H_2O	
3	500–630	H_2O, CO_2		H_2O, CO_2	
4	630–700	H_2O, CO_2		CO_2, O_3	
5	700–820	H_2O, CO_2	CCl_4	CO_2, O_3	CCl_4
6	820–980	H_2O	CO_2, CFC-11,‡ CFC-12	···	CFC-11,‡ CFC-12
7	980–1080	H_2O, O_3	CO_2	O_3	
8	1080–1180	H_2O	CO_2, CFC-12, CFC-22‡	O_3	
9	1180–1390	H_2O, CH_4		CH_4	
10	1390–1480	H_2O		H_2O	
11	1480–1800	H_2O		H_2O	
12	1800–2080	H_2O, CO_2		···	
13	2080–2250	H_2O, N_2O		···	
14	2250–2380	CO_2		CO_2	
15	2380–2600	N_2O, CO_2		···	
16	2600–3000	H_2O, CH_4		···	

*1050–96 mbar except for band 8 (1050–317 mbar).
†96–0.01 mbar except for band 8 (317–0.01 mbar).
‡Optical depths of these halocarbons are increased to account for other absorption bands of these species that are not implemented.

(Mlawer *et al.* 1997)

RRTM Development Strategy

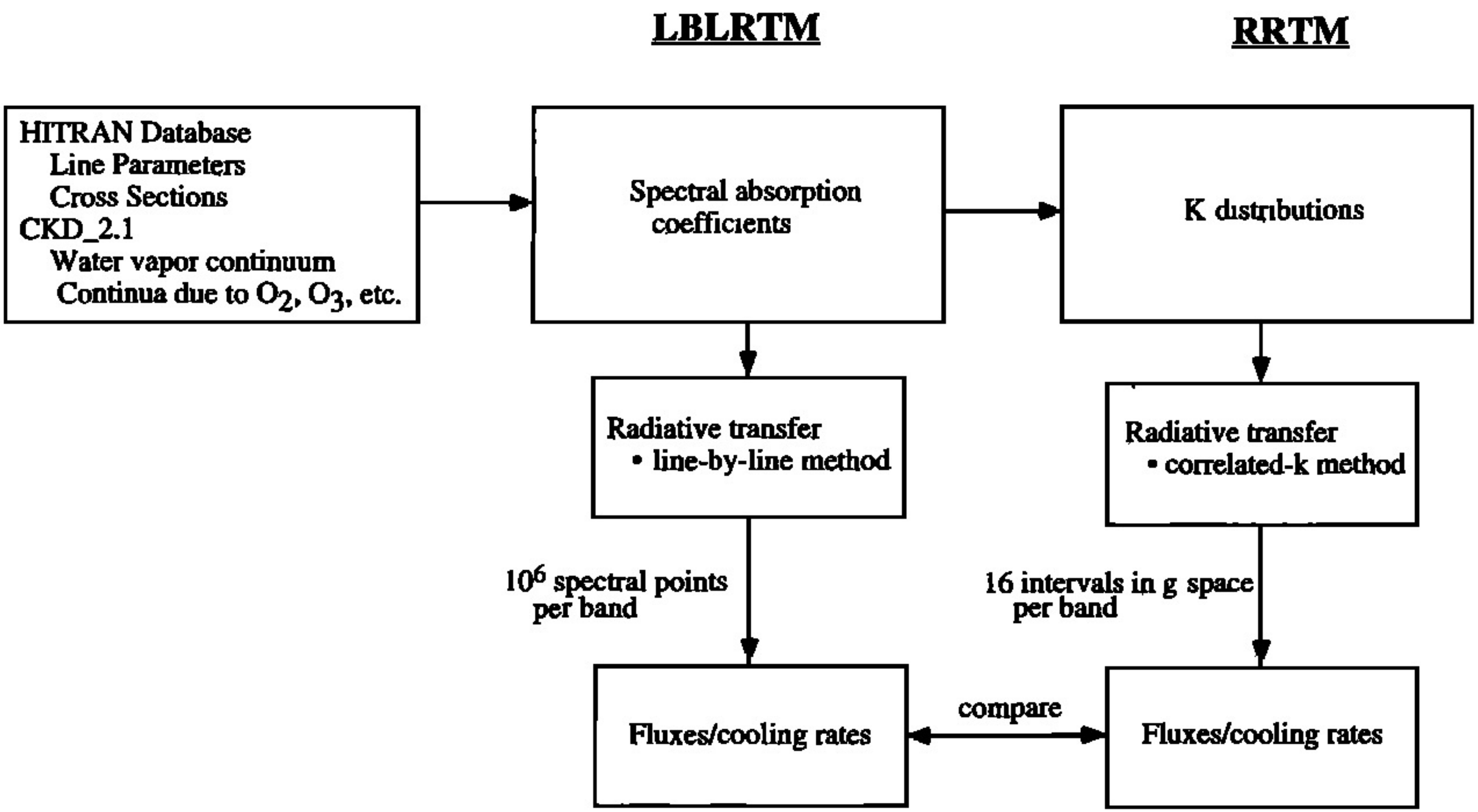

Figure 2. Developmental strategy of RRTM.

(Mlawer *et al.* 1997)

Gallus & Bresch – rainfall forecast sensitivity

- Gallus and Bresch (2006) examined rainfall forecast sensitivity as a function of model physics, dynamics, and initial conditions in simulations of 15 rainfall events in the central U.S. during August 2002.

- Two dynamical cores and two physics packages were used in a total of four configurations that were all initialized with ETA output. Dynamical cores used were the nonhydrostatic mesoscale model (NMM) and the Advanced Research WRF (ARW).

Physics packages

- The first physics package (NCEP) used the Betts-Miller-Janic convection scheme, GFDL radiation package, and Mellor-Yamada-Janic PBL scheme.

- The second physics package (NCAR) incorporated the Kain-Fritsch convective scheme, Dudhia rapid radiative transfer model (RRTM), and Yonsei University PBL scheme. Additional physical schemes (e.g. Ferrier *et al.* microphysics, Noah land surface model) were identical in all runs. Simulations were performed at 8-km grid spacing with 60 vertical layers, using 1200 UTC ETA 40-km Gridded Binary (GRIB) output for initial and lateral boundary conditions (Gallus and Bresch 2006).

Precipitation results

- Results indicate that NCAR physics with both dynamic cores generally overestimated peak rain rates, and 3 show a 12–18-h forecast period for WRF runs and observations respectively, indicating greater intensity and finer structure from the NCAR physics (Gallus and Bresch 2006).

- Each of the simulations has significant differences from the observations. Gallus and Bresch (2006) concluded that peak rain rate sensitivity is more a function of physics package than dynamic core, while total rain volume is more a function of dynamics than physics. The two radiation schemes did not cause notable differences.

Observed rainfall

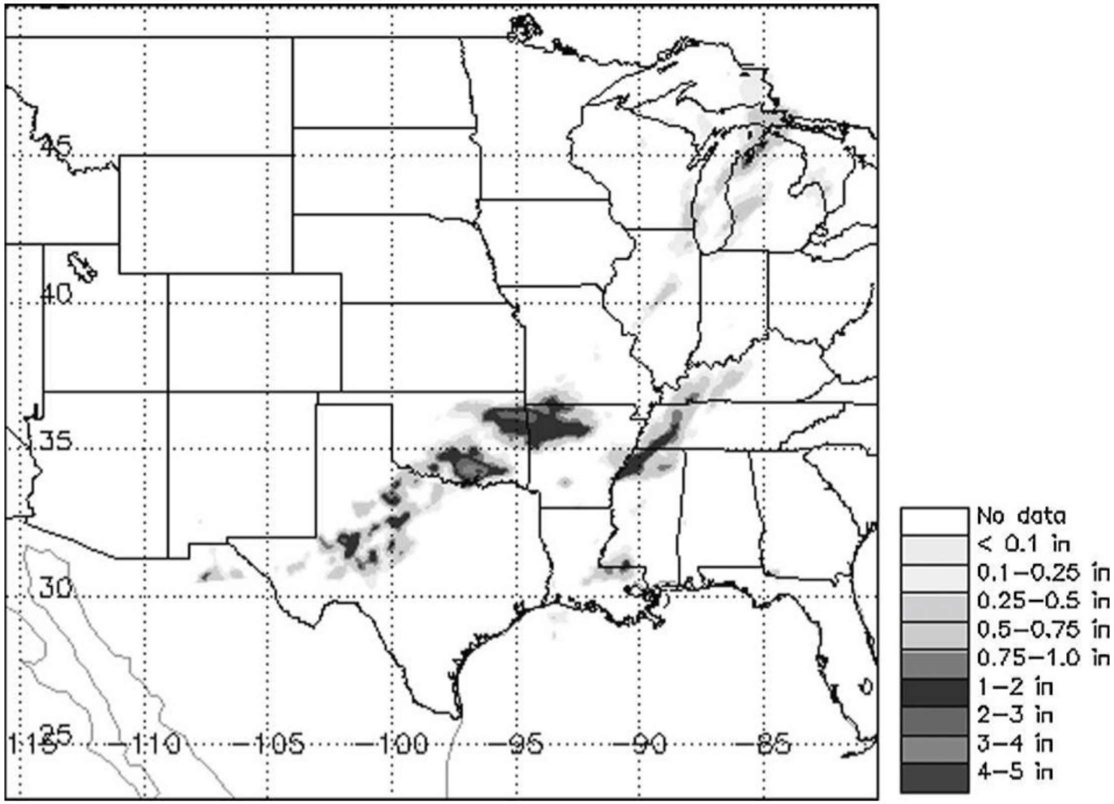

FIG. 2. Observed rainfall (from stage-IV multisensor analysis) in the 0000–0600 UTC period on 14 Aug 2002 corresponding to the 12–18-h forecast period in the runs shown in Fig. 1.

(Gallus and Bresch 2006)

Rainfall simulations

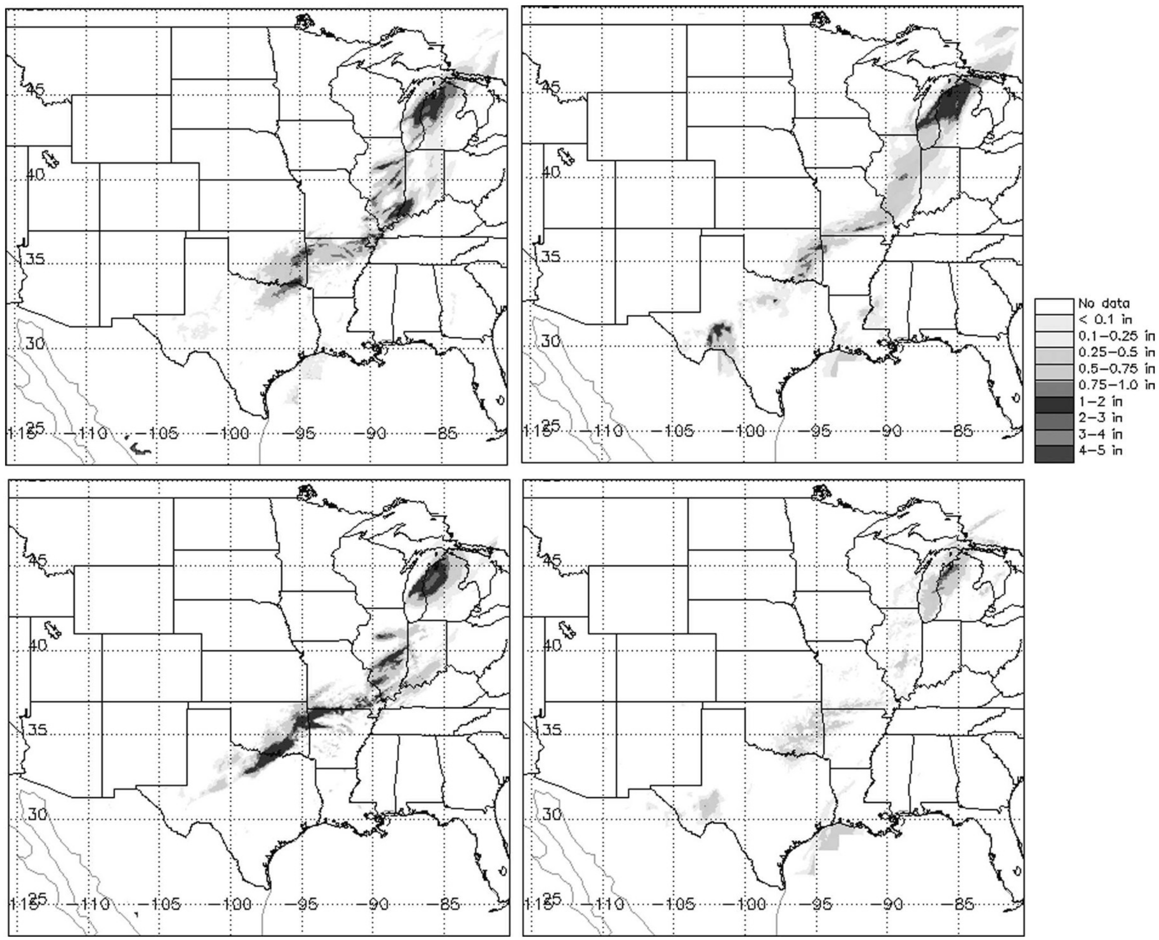

FIG. 1. Rainfall in the 12–18-h forecast period (0000–0600 UTC 14 Aug 2002) for a case initialized at 1200 UTC 13 Aug 2002. Runs using (top) ARW dynamic core and (bottom) NMM; (left) NCAR physics and (right) NCEP.

(Gallus and Bresch 2006)

Evaluation of parameterizations

- The ability to use different configurations of parameterization schemes is a strong point for WRF. This allows researchers to juxtapose different combinations and thus better evaluate individual and combined schemes.

- Parameterization schemes are constantly evolving, and although the ones identified in this presentation represent significant improvements over previous versions, they have the inherent limitations of the era in which they were developed.

Future development

- The new version of the Goddard scheme illustrates this. The new Goddard scheme has a correct two-stream adding approximation in diffuse transmissivity, while the old scheme had an incorrect diffuse transmissivity – a critical bug in the code.

- The new scheme uses delta-Eddington approximation for reflection and transmittance of direct and diffuse radiation, while the old uses delta-Eddington approximation for direct radiation, but it uses equations in Sagan and Pollock (JGR, 1967) for diffuse radiation.

References

Chen, S.H. and Dudhia, J., 2000: Annual report: WRF physics. *Air Force Weather Agency*, **38**.

Dudhia, J., 1989: Numerical study of convection observed during the winter monsoon experiment using a mesoscale two-dimensional model. *J. Atmos. Sci.*, **46**, 3077–3107.

Gallus Jr., W. A., J. F. Bresch, 2006: Comparison of impacts of WRF dynamic core, physics package, and initial conditions on warm season rainfall forecasts. *Mon. Wea. Rev.*, **134**, 2632–2641.

Lacis, A. A., and J. E. Hansen, 1974: A parameterization for the absorption of solar radiation in the Earth's atmosphere. *J. Atmos. Sci.*, **31**, 118–113.

Liou, K.-N, 1980: An Introduction to Atmospheric Radiation. Academic Press.

Mlawer, E. J., S. J. Taubman, P. D. Brown, M. J. Iacono, and S. A. Clough, 1979: Radiative transfer for inhomogeneous atmospheres: RRTM, a validated correlated-*k* model for the longwave. *J. Geophys. Res.,* **102**, 16,663–16,682.

Sagan, C., and J. B. Pollack, 1967: Anisotropic nonconservative scattering and the clouds of Venus. *J. Geophys. Res*. **72**, 469-477.

References

Skamarock, W. C. *et al.,* 2007: A Description of the Advanced Research WRF Ver. 2. *NCAR Tech. Note* NCAR/TN–468+STR, 88 pp.

Stensrud, D. J., 2007: Parameterization Schemes: Keys to Understanding Numerical Weather Prediction Models. Cambridge University Press, 459 pp.